Formation of Polymorphic Structure and Its Influences on Properties in Uniaxially Stretched Polybutylene Terephthalate Films

KWANGJIN SONG

Department of Mechanical Engineering, Yale University, P.O. Box 208286, New Haven, Connecticut 06520-8286

Received 17 April 1999; accepted 4 February 2000

ABSTRACT: The evolution of structure and properties in uniaxially stretched polybutylene terephthalate (PBT) films has been explored. The stretch temperature has pronounced influences on the development of PBT polymorphism; the mechanisms of its formation involve levels of both applied stress as well as chain relaxation during the stretch period. The stretch rate, on the other hand, tends to perfect the structure. PBT films produced under different conditions develop different levels of crystallinity and orientation in the individual α and β phases, in which annealing under tension induces a partial crystal transition from the β to α phase that leads to an increment of orientation in the α phase. The mechanical behavior of the films is related to the polymorphic structure as well as to the overall chain orientation. © 2000 John Wiley & Sons, Inc. J Appl Polym Sci 78: 412–423, 2000

Key words: polybutylene terephthalate (PBT); uniaxial films; polymorphism; orientation; property

INTRODUCTON

Polybutylene terephthalate (PBT) is a thermoplastic polyester used for many engineering applications such as injection molding, extrusion, and as a component of polymer composites and alloys; the molecule has four flexible methylene groups and a hard segment of a terephthalate group in its repeating unit. The crystalline structures of PBT have received considerable study.[1–23] Two different crystalline forms designated as the α and β forms and a smectic glassy state have been identified. The α-form crystalline structure that is found in a relaxed state is the most stable, in which the chain involves the glycol residue in a *gauche-trans-gauche* (gtg) conformation. When the α-PBT is held under strain, the β-form crystal arises through a crystal–crystal transition, which contains the glycol residue in an all *trans* (ttt) conformation.

In 1974, Boye and Overton[1] first observed that PBT undergoes a reversible crystal–crystal phase transition with uniaxial drawing. Subsequently, several studies of crystalline structures have been reported in the literature,[2,3,6–9,11,18,19,23] where the α-form structures are generally in agreement. However, a controversy has arisen concerning the β structure. Mencik[2] was the first who indexed a unit cell of the α-PBT, which is triclinic with $P\bar{1}$ space group and has lattice parameters of a = 4.83 Å, b = 5.96 Å, c = 11.62 Å, α = 99.9°, β = 115.2°, and γ = 113.8°. This α-form structure identified by Mencik was confirmed later by many investigators.[9,11,18,23] The β unit cell is also triclinic with $P\bar{1}$ space group.[4,8,14] In the strain ranges of 4–20%, the α-PBT is transformed into the β crystal due to lattice extension. Yokouchi et al.[6] proposed that the α crystal has ca. 68° inter-

Correspondence to: K. Song (kwangjin.song@yale.edu).

Journal of Applied Polymer Science, Vol. 78, 412–423 (2000)

nal rotation of the methylene bonds, with the terephthalate residue being nonplanar to the carbonyl bonds, and that a β structure holds dimensions of a = 4.73 Å, b = 5.75 Å c = 13.11 Å, α = 104.2°, β = 120.8°, and γ = 100.9°. Hall and Pass,[7] however, claimed that the α crystal has 77° internal rotation of methylene bond, with terephthalate residue being planar to the carbonyls, and they also proposed a different β crystal that has dimensions of a = 4.69 Å, b = 5.80 Å, c = 13.00 Å, α = 101.9°, β = 120.5°, and γ = 105.0°. The large discrepancy between these two β-form structures was explained in terms of characteristics of PBT wide angle X-ray scattering (WAXS) patterns that exhibited blurred reflections of the $(\bar{1}\ 10)\beta$ and $(100)\beta$ planes.[9]

Many polymers exhibit polymorphism that is characterized by the tendency for a polymer to crystallize into more than one conformational state; its development is found to depend greatly on processing history and molecular mechanism of the polymer.[24–27] Melt-spinning and cold-drawing of PBT induced a metastable β phase being retained in resultant fibers,[12,18,28–31] in which increasing draw ratio perfected the β crystal, the relative fraction of which had effects on mechanical properties of the fibers. PBT tapes that were prepared by free width uniaxial drawing also exhibited the α- and β-form crystals,[32,33] where their formation was dependent greatly on the processing temperature. In film processing, however, there have been few studies on the development of PBT structure and its relationships to properties.[34,35] In the present work, we investigate the evolution of PBT polymorphism and its influences on properties in uniaxial films stretched at constant width; the deformation behavior of the individual phases is related to the development of chain orientation and to the physical properties of resultant films.

EXPERIMENTAL

Materials and Film Formation

The polymer used in this study was PBT, Ultradaur KR4036-Q692 of BASF Corporation (USA). The PBT pellets having an intrinsic viscosity of 1.24 dℓ/g were dried at 110°C overnight in a laboratory vacuum oven, and then fed into a 25-mm Prodex single screw extruder that was equipped with a 203-mm-wide coater hanger die and a chilled roll take-up unit. The polymers were extruded at 260°C through the shaping die, and then cooled on the chilled roll, producing PBT cast sheets with a thickness ca. 300 μm, which were largely glassy in nature. The sheets were cut into dimensions of 12 × 12 cm, placed inside the chamber of an Iwamoto film stretcher (Model BIX-702), and then gripped by 40 pneumatic clips. The stretch temperatures were respectively 45, 65, 90, 125, and 160°C. After 1 min equilibrium at the prescribed temperature, the sheets were uniaxially stretched to 400% at constant width, i.e., the stretch ratio (λ_{MD}) along the machine direction (MD) × the stretch ratio (λ_{TD}) along the transverse direction (TD) = 4 × 1, with initial strain rates (v/L_o) of 0.5 and 0.2 s^{-1} (v: the stretch speed; L_o: the initial length of the sheet). The stretched films were immediately cooled down, while maintaining the stress, to room temperature by using a cold air blower. Selected films stretched at 90°C were subsequently fixed annealed at 150°C for 8 hr in the biaxial stretcher.

WAXS Diffraction

WAXS diffraction measurements were performed using Rigaku and GE X-ray diffractometers. A nickel foil filter was used to obtain CuKα radiation. The films were stacked with epoxy glue and cut into dimensions of 20 × 20 × 1.2 mm. WAXS flat film photographs were taken along the three orthogonal directions of the specimen: through, edge, and end view patterns,[36] and the samples were 2θ scanned over the Bragg angles from 5 to 60°. Pole figures were constructed for several lattice planes to understand the crystalline orientation. The samples with dimensions of 1.2 × 15 × 1.2 mm were mounted on a single crystal orienter with their MD as the spindle axis. The diffraction intensities were collected around two Eulerian angles at intervals of χ of 5° and ϕ of 10°.

The α- and β-form unit cells of Hall and Pass[7] were used to identify crystalline reflections in the films. A curve resolution method using Pearson VII function was applied to separate the overlapped peaks,[37,38] and then mean crystal sizes (D_{hkl}) for the individual phases were estimated using Scherrer equation. Because higher order reflections were not measurable in PBT, no correction for distortion broadening was applied; only relative crystal sizes were obtained for the comparison of samples produced under different conditions. The relative fraction of β-PBT (X_β) was also determined following an approximation method proposed by Turner–Jones et al.[39]

$$D_{hkl} = \frac{f\lambda}{(\Delta\theta_{1/2}^2 - \Delta\theta_{inst}^2)^{1/2}} \frac{1}{\cos\ \theta_{hkl}} \quad (1)$$

$$X_\beta = \frac{I_{\bar{1}06\beta}}{I_{\bar{1}06\beta} + \kappa(I_{100\alpha} + I_{010\alpha})} \quad (2)$$

where λ is the wavelength (1.542 Å) of the X-ray, $\Delta\theta_{1/2}$ and $\Delta\theta_{inst}$ are respectively the peak breadth at half-maximum intensity and the instrumental broadening, θ_{hkl} is the Bragg angle, I is the peak intensity, and κ is a proportionality constant.

Pole figures of the off-meridional $(\bar{1}\ 04)\alpha$ and $(\bar{1}\ 06)\beta$ planes were used to quantify orientation in the individual phases. The second moments of the orientation distribution have been determined by applying Wilchinsky's treatment[40]:

$$\overline{\cos^2\phi_j} = \frac{\int_0^{2\pi}\int_0^{2\pi} I_{hkl}(\phi_1, \chi_1)\cos^2\phi_1 \sin\ \phi_1\, d\phi_1\, d\chi_1}{\int_0^{2\pi}\int_0^{2\pi} I_{hkl}(\phi_1, \chi_1)\sin\ \phi_1\, d\phi_1\, d\chi_1} \quad (3)$$

where $I_{hkl}(\phi_1,\chi_1)$ is the diffracted intensity distribution in the pole figures. White–Spruiell biaxial crystalline orientation factors[41] are then computed through:

$$f_{1,j}^B = 2\overline{\cos^2\phi_{1,j}} + \overline{\cos^2\phi_{2,j}} - 1 \quad (4a)$$

$$f_{2,j}^B = 2\overline{\cos^2\phi_{2,j}} + \overline{\cos^2\phi_{1,j}} - 1 \quad (4b)$$

where $\phi_{i,j}$ is the angle between film direction i and crystallographic axis j.

Refractive Index

Refractive indices and birefringences of the films were obtained using a Bellingham Stanley Abbe 60/HR refractometer with a polarizing eyepiece. A monochromatic sodium lamp of wavelength 589.6 nm was used as a light source and diiodomethane sulfur (n_D = 1.75) as an immersion liquid. The sample with dimensions of 40 × 40 mm was placed on the prism with its MD either parallel or perpendicular to the long axis of the measuring prism. Two refractive indices, n_{MD} and n_{ND} or n_{TD} and n_{ND}, were then respectively read. From refractive indices, birefringences (Δn_{13},Δn_{23}) were determined by:

$$\Delta n_{13} = n_1 - n_3 \quad (5a)$$

$$\Delta n_{23} = n_2 - n_3 \quad (5b)$$

where "1" is the MD, "2" is the TD, and "3" is the normal direction (ND).

Tensile Testing

Tensile testing was performed using an Instron Tensometer Model 4204 at room temperature. The span length and the rate of stretching were set respectively at 25 mm and at 25 mm/min. Films were cut into 0.6 × 7.0 cm along the MD and TD. Five samples were tested at each condition and the measured results were averaged.

RESULTS

WAXS Flat Film Photographs

In general, uniaxial PBT films revealed distinct crystalline arcs in WAXS flat film photographs (Fig. 1). At a strain rate (v/L_o) of 0.2 s^{-1}, the patterns through the '13' plane comprised intense $(001)\alpha$ spots on the first layer line, with blurred scattering on the equator. As the stretch speed increased, the reflections tended to strengthen. The patterns varied substantially with stretch temperature. At a temperature 45°C, the equatorial arcs, which were diffuse, were superposed by strong amorphous scattering, and on the first layer line that was close to the meridian, a weak reflection through the '13' plane was discernible. The Debye spots evolved into arcs with an increase of the temperature, resulting in a number of α reflections that were markedly intensified on the azimuth. In the end pattern, on the other hand, a spot close to the meridian on the second layer line became increasingly circular with an increase of the stretch temperature.

WAXS Diffractometer Scans

Figure 2 shows that in WAXS 2θ scans, the diffracted peaks varied substantially with stretch temperature. At a temperature 45°C, the meridional diagrams contained a peak at 'd' spacing 11.69 Å and two β reflections of an intense $(\bar{1}\ 06)$ peak and a detectable $(\bar{1}\ 04)$ peak, where the peaks revealed few changes with the scan direction [Fig. 2(a)]. As the stretch temperature increased, the α peaks arose on the meridian, developing anisotropy. At 160°C, the diffractograms

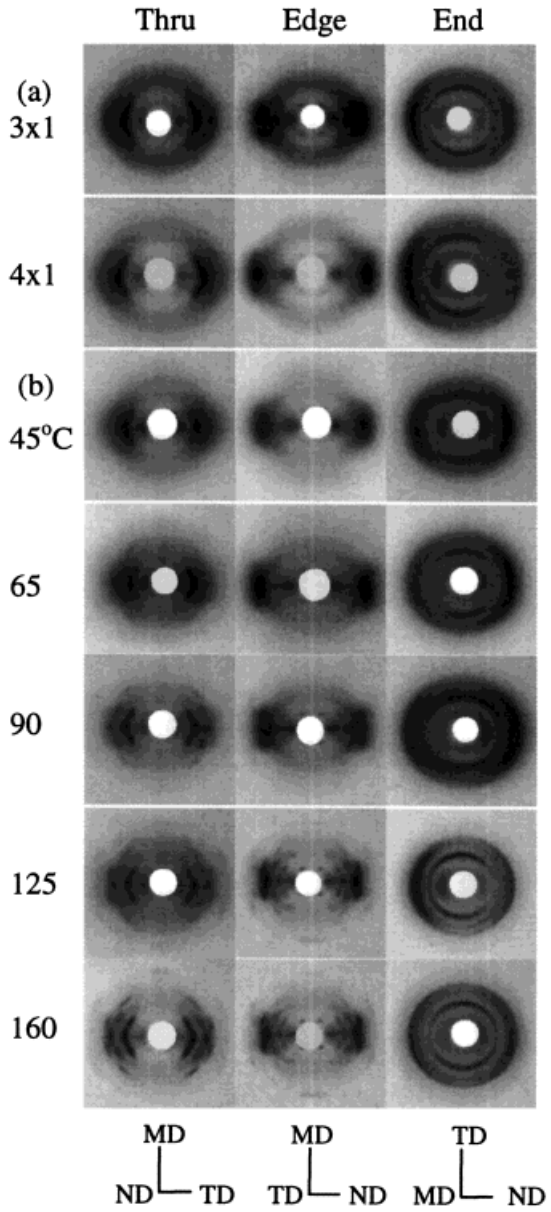

Figure 1 WAXS flat film photographs of PBT films uniaxially stretched at constant width; (a) films stretched at 90°C and 0.2 s^{-1} as a function of stretch ratios, $\lambda_{MD} \times \lambda_{TD}$, (b) films stretched at $\lambda_{MD} \times \lambda_{TD} = 4 \times 1$ and 0.5 s^{-1} as a function of stretch temperature.

disclosed intense $(\bar{1}\ 04)\alpha$ and $(\bar{1}\ 05)\alpha$ peaks, with weak reflections of the (001) plane and β phase. In equatorial scans [Fig. 2(b)], on the other hand, the (010) and (100) peaks were distinct; however, they became broadened at low temperatures $\leq$65°C. An increase of the stretch temperature caused the $(010)\alpha$ and $(100)\alpha$ peaks to strengthen respectively in the through and edge scans, in which the (100) peak revealed slight variations in

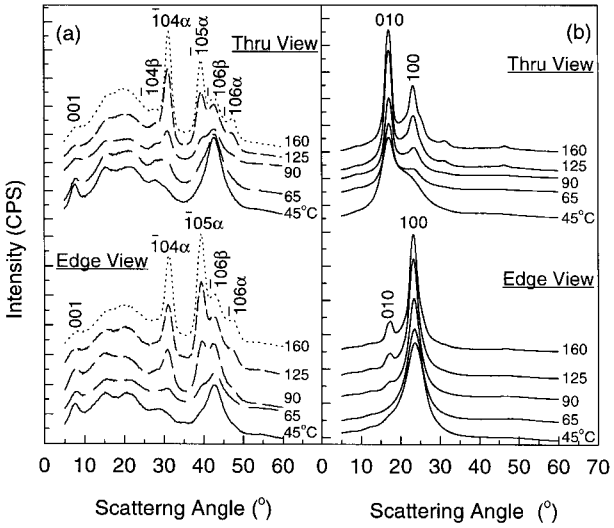

Figure 2 WAXS 2θ scans of PBT films uniaxially stretched at $\lambda_{MD} \times \lambda_{TD} = 4 \times 1$ and 0.5 s^{-1} as a function of stretch temperature; (a) meridional scans, (b) equatorial scans.

its position. Figure 3 presents 2θ through scans as a function of azimuthal angle; the incident X-ray beam was parallel to the normal direction. In unannealed films [Fig. 3(a)], the (100) and (010) peaks appeared within 11° from the equator ($\chi = 90°$) and the highest $(0\bar{1}\ 1)\alpha$ peak at $\chi \cong 67.5°$; on the other hand, several off-meridional reflec-

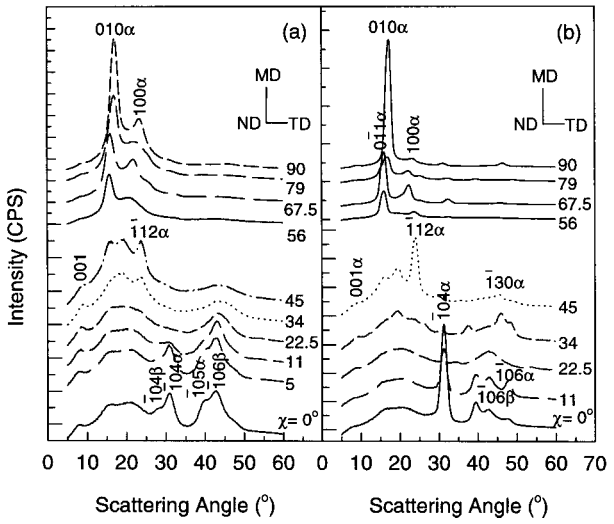

Figure 3 WAXS 2θ scans of PBT films as a function of azimuthal angle; (a) films uniaxially (4 × 1) stretched at 90°C and 0.5 s^{-1}, (b) films uniaxially (4 × 1) stretched at 90°C and 0.5 s^{-1} and then subsequently fixed annealed at 150°C for 8 h.

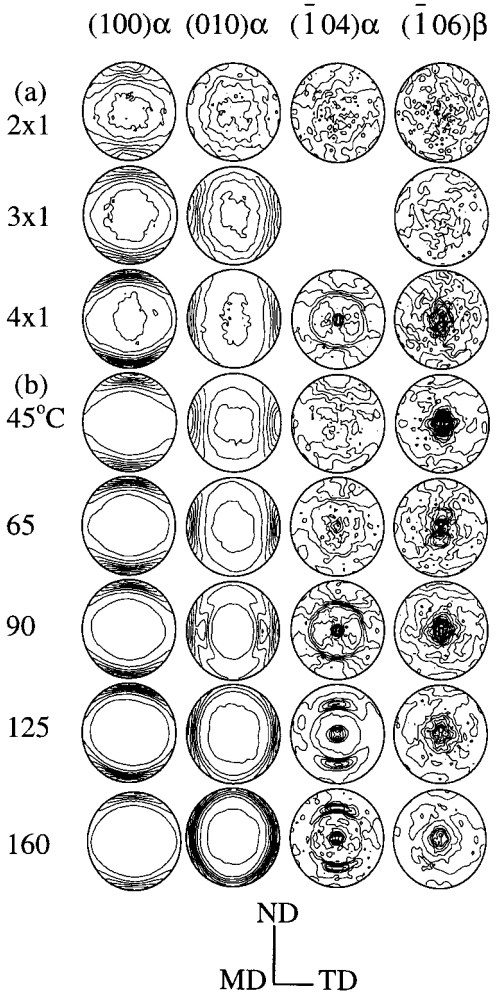

Figure 4 WAXS pole figures of PBT films uniaxially stretched under various stretch conditions; (a) films stretched at 90°C and 0.2 s^{-1} as a function of stretch ratios, $\lambda_{MD} \times \lambda_{TD}$, (b) films stretched at $\lambda_{MD} \times \lambda_{TD} = 4 \times 1$ and 0.5 s^{-1} as a function of stretch temperature.

tions were recorded within 11° from the meridian. Upon annealing [Fig. 3(b)], both the (010)α and ($\bar{1}$ 04)α peaks intensified substantially, but the (100)α peak on the equator weakened; on the meridian, the ($\bar{1}$ 04)β peak vanished, however the ($\bar{1}$ 06)β peak, though weak, still persisted.

WAXS Pole Figures

For a given stretch temperature of 90°C [Fig. 4(a)], an increase both in stretch ratio and strain rate strengthened plane normals of both the α and β phases. The poles of the (100)α and (010)α planes tended to focus respectively on the ND and TD while the ($\bar{1}$ 04)α and ($\bar{1}$ 06)β pole figures comprised the highest intensity in the MD. The pole figures displayed changes with varying stretch temperature [Fig. 4(b)]. As the temperature increased, the (010) poles spread in the TD-ND plane, while the ($\bar{1}$ 04)α poles, which exhibited very weak concentrations at temperatures $\leq$65°C, increasingly intensified in the MD. The ($\bar{1}$ 06)β poles, on the other hand, tended to weaken with increasing of the stretch temperature.

Refractive Indices

The optical properties of PBT films are plotted in Figure 5. A film stretched at v/L_o = 0.2 s^{-1} and 90°C had n_{MD} = 1.6792 and n_{TD} = 1.5585; these values were smaller than those found in a corresponding film stretched at a higher strain rate 0.5 s^{-1}. The refractive indices increased with rising stretch temperature; however, variations in n_{MD} and n_{TD} were marginal, which resulted in an $\bar{n}$ = 1.57253 at 45°C and an $\bar{n}$ = 1.58816 at 160°C. Birefringences (Δn_{13},Δn_{23}) showed an opposite tendency; they reduced with increasing stretch temperature, indicating that the films stretched at high temperatures have more disoriented polymer chains. A uniaxially stretched film at 45°C exhibited the maximum birefringences of Δn_{13} = 0.187 and Δn_{23} = 0.106.

The optical properties of annealed films are presented in Figure 6 as a function of annealing time (t_a). The n_{MD} continued increasing with lengthening $t_a \leq$ 10 h and then leveled off with further annealing. The n_{TD} and n_{ND} showed a rapid increase at t_a below 1 h. The annealed films revealed much higher birefringences with a maximum $\Delta n_{13} \cong$ 0.2053, where a rapid increase in Δn_{13} and Δn_{23} was also registered at t_a below 1 h.

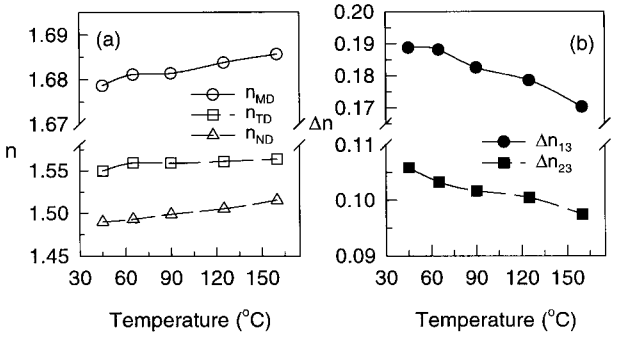

Figure 5 Optical properties of PBT films uniaxially stretched at $\lambda_{MD} \times \lambda_{TD} = 4 \times 1$ and 0.5 s^{-1} as a function of stretch temperature; (a) refractive indices (n), (b) birefringences (Δn).

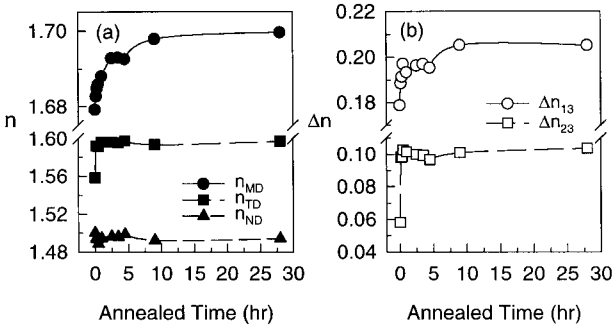

Figure 6 Optical properties of PBT films uniaxially (4×1) stretched at 90°C and 0.5 s^{-1} and then fixed annealed at 200°C with different time intervals; (a) refractive indices (n), (b) birefringences (Δn).

Mechanical Properties

Figure 7 presents the stress-strain curves for PBT films that were uniaxially stretched at $\lambda_{MD} \times \lambda_{TD} = 4 \times 1$. A plateau region occurred at strains of 4 to 15% and tended to lengthen with increasing of the stretch temperature. However, at strains $\leq$5%, i.e., below the onset of the plateau, stress increment decreased with rising temperature. A marked plateau region was seen at high stretch temperatures $\geq$125°C. Figure 8 shows that the Young's modulus and tensile strength increased in the direction of stretch while the elongation to break reduced. The stretch temperature noticeably influenced on mechanical property; increasing temperature reduced the MD modulus while it progressively increased the MD tensile strength. The elongation to break, however, was very low and remained relatively constant. At right angles, the mechanical properties generally showed a reverse tendency, with little variations in TD strength. A film stretched at 45°C exhibited the highest MD Young's modulus of 3.81 GPa.

DISCUSSION

Polymorphic Structure

PBT films that were uniaxially stretched at $\lambda_{MD} \times \lambda_{TD} = 4 \times 1$ exhibited two different crystalline structures, an observation which is consistent with what was seen in fibers.[22,28–31] The β-PBT tended to develop more in the films that were produced at lower stretch temperatures $\leq$65°C. As the applied stress decreased, the polymer chains were increasingly in the relaxed conformation, producing more α-PBT in resultant films.

The Bragg spacings of various lattice planes were estimated as a function of stretch temperatures (Fig. 9). At low stretch temperatures, the d spacing (d_{100}) of the (100) plane revealed intermediate values between those of the α and β planes, suggesting the presence of polymorphic structures. The d_{100} was found to decrease from 3.79 to 3.62 Å with an increase of the β crystallinity.[14] However, changes in processing conditions caused little variations in d spacings of the off-meridional planes. A reflection that occurred close to the (001) Bragg angle showed temperature-dependent d spacings; at a stretch temperature 45°C, the peak appeared at a d spacing of ca. 11.69 Å that is identical with the chain repeat distance of the α phase. As the stretch temperature increased, the d spacing gradually reduced to that of the (001)α plane. This reflection occurring at lower temperatures, which tended to disappear with annealing, may result from a highly oriented smectic phase present in the as-stretched films, as observed in other polyesters such as polyethylene terephthalate and polyethylene naphthalate.[42–46]

Crystal Size and Phase Content

PBT films produced at stretch temperatures $\leq$90°C revealed diffuse scattering on the equator, presumably due to both crystal imperfection as well as reflection overlap of the α and β planes. As the separation in 2θ angles of the (100) and (010) planes of the two crystalline phases is very small

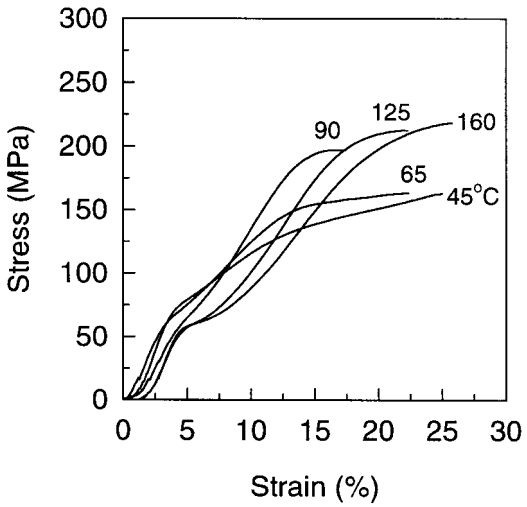

Figure 7 Stress-strain curves for PBT films uniaxially stretched at $\lambda_{MD} \times \lambda_{TD} = 4 \times 1$ and 0.5 s^{-1} as a function of stretch temperature.

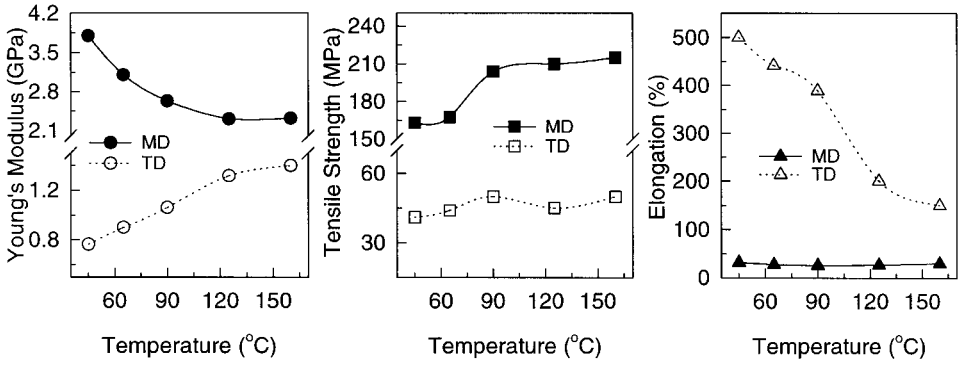

Figure 8 Mechanical properties of PBT films uniaxially stretched at $\lambda_{MD} \times \lambda_{TD} = 4 \times 1$ and 0.5 s^{-1} as a function of stretch temperature.

below 1.5°, these reflections tend to overlap and need to be separated to estimate the size and content of the individual crystals. In cold-drawn PBT fibers and tapes,[10,22,28,31] the ($\bar{1}$ 04) and ($\bar{1}$ 06) peaks of the α and β phases were found to be intense and used to estimate the relative fraction of the individual phases. In PBT films that were uniaxially stretched at constant width, however, only the ($\bar{1}$ 06)β peak was strong on the meridian, probably due to the biaxial nature of applied stress, which tended to result in rather imperfect crystals. The content of each phase was, therefore, approximated using Eq. (2) and the results are given in Table I.

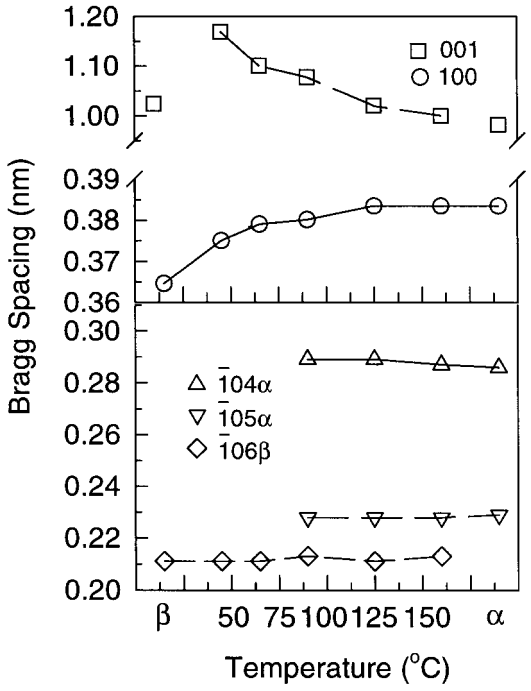

Figure 9 Bragg spacings of PBT lattice planes for uniaxial films stretched at $\lambda_{MD} \times \lambda_{TD} = 4 \times 1$ and 0.5 s^{-1} as a function of stretch temperature.

As expected, the stretch temperature had profound effects on the perfection and relative fraction of the α and β phases. An increase in temperature thickened the crystal dimensions of the α-PBT while it reduced the β crystal sizes. A uniaxial film stretched at 45°C had $D_{010\alpha}$ = 23 Å and $D_{\bar{1}\,06\beta}$ = 22 Å, with a relative fraction ca. 60% of the β-PBT (X_β). Å much higher fraction (X_β) 91% of the β phase was reported in a fiber cold-drawn at 22°C.[28] Films stretched at high temperatures ≥125°C revealed substantially low β crystallinity having an $X_\beta \cong 9\%$. In addition, the content of the β phase changed little with time; a film that was stored for 1 year at room temperature was found to retain the β crystallinity whose fraction was similar to that determined from the precursor film before storage. It appears that the β crystals, once formed in the films, are very

Table I Crystal Sizes (D_{hkl}) and the Relative Fractions (X_β) of the β Phase for PBT Films Uniaxially Stretched at $\lambda_{MD} \times \lambda_{TD} = 4 \times 1$ and 0.5 s^{-1} as a Function of Stretch Temperature

Temperature (°C)	D_{hkl} (Å)				
	010α	100α	$\bar{1}$04α	$\bar{1}$06β	X_β (%)
45	23.2	10.7		21.5	59.7
65	32.9	13.9		19.7	40.8
90	40.8	17.8	39.5	18.3	25.1
125	48.3	23.5	43.1	16.1	15.2
160	46.8	26.2	50.7	16.3	8.96

stable. Annealing under tension, on the other hand, induced a partial $\beta \rightarrow \alpha$ crystal transformation, probably owing to relaxation of the internal stress.

Formation of a Stable β Phase

During the stretch process, the undrawn PBT sheets underwent internal changes associated with the preheating period before stretch. This preheating process at low stretch temperatures may induce smectic α ordering in the film by the chain motion under low stress conditions. Subsequently, with stretching, the β crystals that have small sizes may arise through the extended-chain crystallization and/or the $\alpha \rightarrow \beta$ crystal transition of the imperfect α ordering. At high stretch temperatures, however, the undrawn sheets went through considerable amounts of α crystallization, as an undrawn sheet preheated at 160°C displayed distinct α reflections. Under such conditions, stretching would induce both crystallization as well as the $\alpha \rightarrow \beta$ crystal transition, in which unstable β crystals may form and revert rapidly back to the α-form crystals on subsequent relaxation, leaving small fractions of the β crystals being retained in resultant films. This stable β crystal, thus, was considered to have lower free energy than required for the crystal transition.[22] It was conjectured that the crystal transition process in PBT was a first-order phase transformation which occurred abruptly at a critical stress that decreased with increasing of the temperature.[12]

Orientation of Crystallites

In highly oriented α-PBT textures, the $(\bar{1}\ 120)$ plane deviates 5.8° from the (100) plane and lies closely normal to the rolled plane that coincides approximately with the $(\bar{2}\ 10)$ plane that is essentially parallel to the phenyl ring plane.[2] This finding generally agrees with what we observed in our experiments, where the $(100)\alpha$ Debye arcs through the '13' plane appeared on the equator and the $(100)\alpha$ poles concentrated primary in the ND. The $(0\bar{1}\ 1)$ plane that appeared off the equator inclined ca. 22° from the c-axis, and the $(001)\alpha$ arcs on the azimuth reflected the tilting character of the α-PBT.[7] The reflections of the $(\bar{1}\ 04)\alpha$, $(\bar{1}\ 05)\alpha$, $(\bar{1}\ 06)\alpha$, and $(\bar{1}\ 06)\beta$ planes that occurred close to the meridian implied that their plane normals lie closely in the 'ab' plane. In oriented α-PBT textures,[6,7] the c-axis tilts 1–2° with respect to the fiber axis, by which the (110) plane remains parallel to the rolled direction and the (310) plane vertical to the tilt. The plane of the phenyl ring inclines about 15° from the fiber axis. In the β conformation,[6–9] on the other hand, the fiber axis tilts 1–5° so that the c axis inclines ca. 86° with respect to the phenyl ring normal.

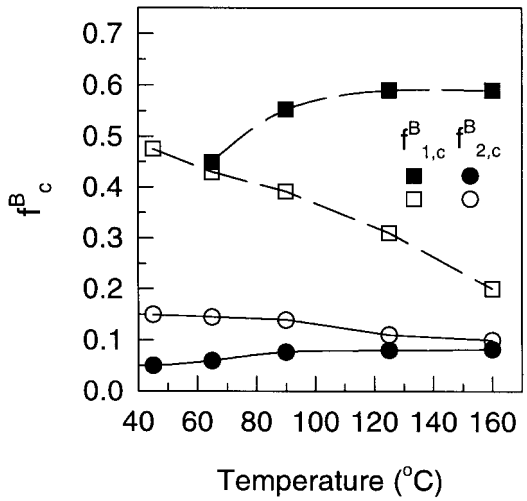

Figure 10 White–Spruiell biaxial orientation factors for PBT films uniaxially stretched at $\lambda_{MD} \times \lambda_{TD} = 4 \times 1$ and 0.5 s^{-1} as a function of stretch temperature; closed symbols: α phase, open symbols: β phase.

Crystalline biaxial orientation factors were computed using Eqs. (4a,b). As presented in Figure 10, the α phase increasingly oriented along the stretch direction (MD) when the stretch temperature was elevated; however, this increment leveled off at temperatures above 90°C probably owing to high degrees of the chain relaxation. The orientation along the TD ($f^B_{1,c}$) varied to a marginal extent with processing. A maximum value of $f^B_{1,c} = 0.61$ suggests highly oriented α-form crystallites present in the films. The β phase, on the other hand, exhibited its highest orientation at a low stretch temperature 45°C, with a maximum value that was considerably lower than that found in the α-form structure. This difference may be due to characteristics of the β-form crystals, which were of small sizes and less perfected.

Refractive Index Versus Crystallinity

Refractive index is a measure of the velocity of the light in the medium and depends on the local density of materials; the property is, thus, related to the crystallinity of the materials. For a two-phase system of crystalline and noncrystalline polymer:

$$\bar{n} = \frac{n_1 + n_2 + n_3}{3} = n_c^o X_c + n_{\text{am}}^o (1 - X_c) \quad (6)$$

where $\bar{n}$ is the mean refractive index, the subscripts 1,2,3 are the three principal directions; n_c and n_{am} are respectively the characteristic refractive indices of the crystalline and amorphous polymer, and X_c is the volume fraction of crystals. The intrinsic birefringences of PBT have been calculated as $\bar{n}_{\alpha}^{o} = 1.628$ for the α-PBT and $\bar{n}_{\beta}^{o} = 1.625$ for the β-PBT,[47] the $\bar{n}_{am}^{o}$ was experimentally determined to be 1.5683.[34] For the α and β-phase, a linear correlation between the mean birefringence and crystallinity was then obtained respectively:

$$\bar{n}_{\alpha} = 5.98 \cdot 10^{-2} \cdot X_c + 1.5683 \quad (7a)$$

$$\bar{n}_{\beta} = 5.67 \cdot 10^{-2} \cdot X_c + 1.5683 \quad (7b)$$

Eqs. (7a,b) can be conveniently used to estimate the X_c of the individual phases from their mean refractive indices that were determined from experiments. For PBT materials having polymorphs, however, it is difficult to separate the contributions of the individual phases to the bulk property. By assuming that the sample consists of only one phase, one may estimate the X_c of the specimen using either of the equations; in this case, Eq. (7a) produces lower X_c's up to 5% than computed from Eq. (7b). The level of this error, however, could be negligible as the PBT samples generally possess low X_c's below 50%. A relationship similar to Eq. (7a) was experimentally achieved for the α-PBT.[34] It is noteworthy that the α- and β-PBT have substantially different values of density; the density of the α-PBT is 1.404 g/cm^3 that is much higher than 1.320 g/cm^3 of the β-PBT.[48] The density of amorphous PBT is 1.282 g/cm^3.[28,49] The crystallinities of PBT samples that possess polymorphic structures, therefore, may reveal uncertainties if determined from density measurements.

Assuming additivity of the properties, we have used Eq. (7a) to obtain the total fraction of crystallites in the films. As noted above, the unannealed films that revealed polymorphs may exhibit slightly lower X_c's than the real values. Figure 11 shows that the estimated X_c's for the annealed films agreed generally with those determined from differential scanning calorimeter measurements.[34] A film stretched at 45°C had an X_c below 10%; the film appears to be largely in a smectic state. The X_c's increased with increasing of the temperature; a film stretched at 160°C had an $X_c \cong 34\%$ that is similar to found in a film annealed at 200°C for 10 min. Obviously, more polymer chains were packed into the α lattices at higher stretch temperatures. The annealed films comprised much higher X_c's, revealing a maximum X_c of ca. 47% at $t_a = 28$ h, in which the crystallinity increased rapidly at the initial stage of annealing. In WAXS measurements, a PBT fiber cold-drawn at 300% and 22°C was found to have 20% X_c,[28] but in density measurements, a PBT tape that was stretched at 350% and 50°C revealed a much lower α crystallinity of ca. 10%, where the density of the β crystal (ρ_{β}) was assumed 1.281 g/cm^3.[32] It seems that stretching of PBT at low temperatures below T_g produces a large proportion of oriented mesophases in resultant samples.

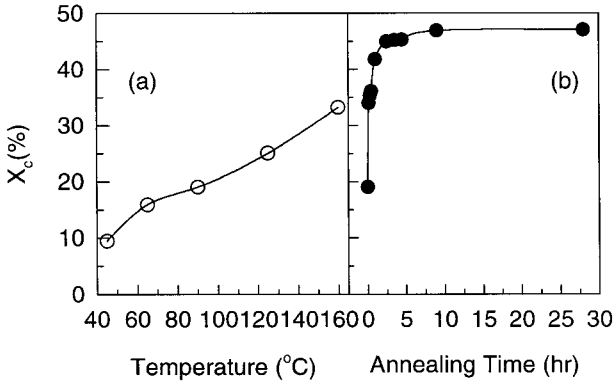

Figure 11 Crystallinities (X_c, %) of PBT films determined from their mean refractive indices; (a) films uniaxially stretched at $\lambda_{\text{MD}} \times \lambda_{\text{TD}} = 4 \times 1$ and 0.5 s^{-1} with different stretch temperatures, (b) films uniaxially (4×1) stretched at 90°C and then fixed annealed at 200°C as a function of duration.

Overall Chain Orientation

Birefringence is a measure of the total molecular orientation of a system. If the Lorentz–Lorenz equation remains valid for oriented polymers, where the polarizability is a second-order tensor, one may write:

$$\frac{\alpha_i - \alpha_j}{\alpha_{11} - \alpha_{\perp}} = \frac{n_i - n_j}{\Delta^o} \quad (8)$$

where

$$\Delta^o = \frac{(\bar{n}^2 + 2)^2}{18\bar{n}} N(\alpha_{11} - \alpha_\perp) \quad (9)$$

Here, n is the refractive index, α is the molecular polarizability, N is the number of molecules per unit volume, Δ^o is the intrinsic birefringence, and $\bar{n}$ is the mean birefringence. Eq. (8) implies that a system increasingly orients with rising of the birefringence $(n_i - n_j)$.

The experiments showed that the overall orientation of the films decreased when the stretch temperature was elevated, whereas it increased with an increase in stretch rate. A film stretched at 45°C that comprised an X_c below 10% revealed the highest Δn_{13} and Δn_{23}, which is obviously related to the noncrystalline chain orientation. At high stretch temperatures, the polymer network must undergo high levels of mobility and relaxation that lead to a large disorientation of the entire chains. Fixed annealing develops stress due to the shrinkage of the film volume, which further stretches the amorphous chains. Therefore, at the initial stage of annealing, i.e., $t_a < 1$ h, the overall orientation increased rapidly which then leveled off with further annealing. This tendency is consistent with the increment of film crystallinity, in which the mechanism seemed to involve phase transitions. It is, thus, expected that constrained annealing of as-stretched PBT films that possess high degrees of the β crystallinity may readily produce films with a high overall orientation.

Mechanical Behavior

Consistent with what has been observed in cold-drawn fibers,[12,28] the inflection of the plateau region in the engineering stress-strain curve became profound with increasing α crystallinity. Films stretched at low extension ratios, $\lambda_{MD} \leq 3$ revealed a distinct yield point, without a plateau region, probably due to a large portion of the amorphous region. As the films increase in orientation and crystallinity, the tensile stress tends to distribute over the crystalline phase, causing the plateau region to emerge. It appears that the variations in plateau length might be due to the local fluctuations of tensile stress over the α structure.

A simple series-parallel model of structural units, in which the tie molecules connect adjacent crystal blocks, can be used to quantitatively explain the effects of degree of structural order and average fraction of taut tie molecules (ξ) on the

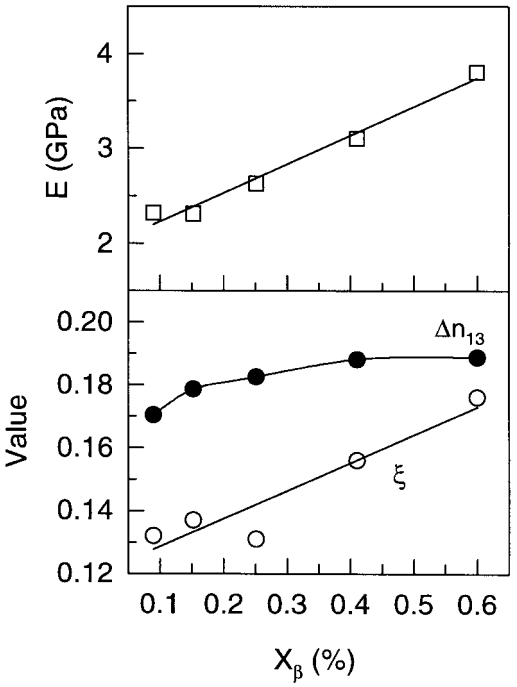

Figure 12 Young's modulus (E), overall chain orientation (Δn_{13}) and fraction of taut tie molecules (ξ) for PBT films uniaxially stretched at $\lambda_{MD} \times \lambda_{TD} = 4 \times 1$ as a function of the fraction of the β-form crystals (X_β).

Young's modulus (E). Assuming a uniform distribution of taut tie molecules over the amorphous region, Peterlin[50] proposed the expression for ξ:

$$\xi = E \frac{(1 - L_c/L_{Long})}{E_c(1 - E(L_c/L_{Long})/E_c)} \quad (10)$$

where, E_c is the axial elastic moduli of crystalline regions, L_c and L_{Long} are respectively the length of crystalline lamella and the long period of crystalline-amorphous alternation. The value of L_c/L_{Long} is roughly equivalent to the crystallinity of the films. The elastic modulus was taken as $E_{c,\beta} = 26.9$ GPa for the β-PBT and $E_{c,\alpha} = 10.1$ GPa for the α-PBT[12]; the values are much smaller than found in polyethylene terephthalate crystal ($E_c = 110$ GPa), the difference of which was attributed to differences in chain conformation between the two polyesters.[51] The fraction of taut tie molecules ξ was then estimated.

As shown in Figure 12, the Young's modulus of the films increased with increasing fraction (X_β) of the β crystals, which also caused an increase in both birefringence and taut tie molecule fraction (ξ). Note that the films having higher birefringences exhibited lower total crystallinities and

lower fractions of the α phase. The mechanical behavior of PBT films, thus, could be complex due to the presence of the three different phases that exhibit different elastic moduli. It appears, however, that the Young's modulus is more closely related to the fraction of the β phase that reveals a high crystal modulus than to the total amount of crystallites. At comparable levels of the overall orientation, on the other hand, the Young's modulus arose as the total crystallinity increased. It was found that the levels of measured moduli were quite low, below 15% of the β-crystal modulus, a behavior that may be explained in terms of the amount and perfection of crystals present in the films. Tensile stretching of PBT films having high fractions of α crystallinity may cause deformation of the α crystals, which, as a result, leads to a large increment of tensile strength.

CONCLUSIONS

The development of polymorphs and properties in uniaxial stretching of PBT films depended greatly on the processing history. A decrease in stretch temperature caused an increase of both the overall chain orientation and the relative fraction of the β phase in resultant films; however, the β-form crystals were imperfect in character with their amounts below 10%. A film produced at a stretch temperature of 45°C was considered to be largely in a mesomorphic state. While increasing stretch temperature $\geq$90°C increased the amount and perfection of the α crystals, it disoriented the entire chain network. An increase of strain rate, on the other hand, tended to produce more ordered polymorphism. A transition from the β- to α-form crystal occurred with fixed annealing that increased the orientation in the α phase as well as in the overall chains. The Young's modulus of the films arose when the β crystallinity was increased, whereas at comparable levels of the overall orientation, the tensile strength depended more on fractions of the α phase, i.e., the total crystallinity. It is, thus, expected that constrained annealing of as-stretched PBT films that possess high fractions of the β-form crystals may readily produce films that reveal high tensile modulus and strength.

The author is greatly indebted to Professor James L. White at the University of Akron for his many useful discussions concerning the subject. He also thanks BASF Co. for supplying the polymer resins investigated in the study.

REFERENCES

1. Boye, C. A.; Overton, J. R. Bull Am Phys Soc 1974, 19, 352.
2. Mencik, Z. J Polym Sci Polym Phys 1975, 13, 2171.
3. Joly, A. M.; Nemoz, G.; Douillard, A.; Vallet, G. Makromol Chem 1975, 176, 479.
4. Jakeways, R.; Ward, I. M.; Wilding, M. A.; Hall, I. H.; Desborough I. J.; Pass, M. G. J Polym Sci B 1975, 13, 799.
5. Ward, I. M.; Wilding, M. A.; Brody, H. J Polym Sci Polym Phys Ed 1976, 14, 263.
6. Yokouchi, M.; Sakakibara, Y.; Chatani, Y.; Tadokoro, H.; Tanaka, T.; Yoda, K. Macromolecules 1976, 9, 226.
7. Hall, I. H.; Pass, M. G. Polymer 1976, 17, 807.
8. Alter, U.; Bonart, R. Colloid Polym Sci 1976, 254, 348.
9. Desborough, I. J.; Hall, I. H. Polymer 1977, 18, 825.
10. Brereton, M. G.; Davies, G. R.; Smith, T.; Ward, I. M. Polymer 1978, 19, 17.
11. Stambaugh, B.; Koenig, J. L.; Lando, J. B. J Polym Sci Polym Phys Ed 1979, 17, 1053.
12. Tashiro, K.; Nakai, Y.; Kobayashi, M.; Tadokoro, H. Macromolecules 1980, 13, 137.
13. Bornschlegl, B.; Bonart, R. Colloid Polym Sci 1980, 258, 319.
14. Alter, U.; Bonart, R. Colloid Polym Sci 1980, 259, 332.
15. Strohmeier, W.; Frank, W. F. X. Colloid Polym Sci 1982, 260, 937.
16. Davidson, I. S.; Manuel, A. J.; Ward, I. M. Polymer 1983, 24, 30.
17. Datye, V. K.; Taylor, P. L. Macromolecules 1985, 18, 671.
18. Perry, B. C.; Koenig, J. L.; Lando, J. B. Macromolecules 1987, 20, 422.
19. Gomez, M. A.; Cozine, M. H.; Tonelli, A. E. Macromolecules 1988, 21, 388.
20. Al-Jishi, R.; Taylor, P. L. Macromolecules 1988, 21, 2240.
21. Grasso, R. P.; Perry, B. C.; Koenig, J. L.; Lando, J. B. Macromolecules 1989, 22, 1267.
22. Roebuck, J.; Jakeways, R.; Ward, I. M. Polymer 1992, 33, 227.
23. Liu, J.; Geil, P. H. J Macromol Sci Phys B36 1997, 2, 263.
24. Seto, T.; Hara, T.; Takana, T. Jpn J Appl Phys 1968, 7, 31.
25. Asada, T.; Onogi, S. In Structure and Properties of Polymer Films; Lenz, R. W.; Stein, R. S., Eds.; Plenum Press: New York, 1973; p. 235.

26. Xenopoulos, A.; Clark, E. S. In Nylon Plastics Handbook; Kohan, M. I., Ed.; Hanser: New York, 1995; p. 108.
27. Phillips, R. A.; Wolkowicz, M. D. In Polypropylene Handbook; Moore, E. P., Ed.; Hanser: New York, 1996; p. 113.
28. Lu, F. M.; Spruiell, J. E. J Appl Polym Sci 1986, 31, 1595.
29. Chen, S. C.; Spruiell, J. E. J Appl Polym Sci 1987, 33, 1427.
30. Chen, S. C.; Spruiell, J. E. J Appl Polym Sci 1987, 34, 1477.
31. Carr, P. L.; Jakeways, R.; Klein, J. L.; Ward, I. M. J Polym Sci Polym Phys 1997, 35, 2465.
32. Kaito, A.; Nakayama, K.; Zubaidi. J Appl Polym Sci 1992, 45, 1203.
33. Zhou, Z.; Cackovic, H.; Schultze, J. D.; Springer, J. Polymer 1993, 34, 494.
34. Song, K.; White, J. L. Polym Eng Sci 1998, 38, 505.
35. Song, K.; White, J. L. Int Polym Proc, to appear.
36. Statton, W. O.; Godard, G. M. J Appl Phys 1957, 28, 1111.
37. Heuvel, H. M.; Huisman, R.; Lind, K. C. J. B. J Polym Sci Phys 1976, 14, 921.
38. Sibila, J. P.; Murthy, N. S.; Gabriel, M. K.; McDonnell, M. E.; Bray, R. G.; Curran, S. A. In Nylon Plastics Handbook; Kohan, M. I., Ed.; Hanser: New York, 1995; p. 70.
39. Tuner–Jones, A.; Aizlewood, J. M.; Beckett, D. R. Makromol Chem 1964, 75, 134.
40. Wilchinsky, Z. W. J Appl Phys 1960, 31, 1969; ibid, Adv X-ray Anal 1963, 6, 231.
41. White, J. L.; Spruiell, J. E. Polym Eng Sci 1980, 20, 247.
42. Bonart, R. Kolloid-Z 1966, 210, 16; ibid, 1966, 213, 1.
43. Asano, T.; Seto, T. Polym J 1973, 5, 72.
44. Auriemma, F.; Corradini, P.; de Rosa, C.; Guerra, G.; Petraccone, V.; Bianchi, R.; Dino, G. D. Macromolecules 1992, 25, 2490.
45. Jakeways, R.; Klein, J. L.; Ward, I. M. Polymer 1996, 37, 3761.
46. Saw, C. K.; Menczel, J.; Choe, E. W.; Hughes, O. R. SPE ANTEC Tech Paper 1997, XLIII, 1610.
47. Ohkoshi, Y.; Nagura, M. Sen-I Gakkaishi 1993, 49, 601.
48. Hall, I. H. Structure of Crystalline Polymers; Elsevier: London, 1984.
49. Stein, R. S.; Misra, A. J Polym Sci Phys Ed 1980, 18, 327.
50. Peterlin, A. In Ultra High Modulus Polymer; Ciferri, A.; Ward, I. M., Eds.; Applied Science Publishers: London, 1979.
51. Thistlethwaite, T.; Jakeway, R.; Ward, I. M. Polymer 1988, 29, 1988.